Sparse Signal Processing Using iterative Method with Adaptive Thresholding (IMAT)

F Marvasti, M Azghani and P Imani, P Pakrouh
ACRI and EE Dept.
Sharif University of Technology
Tehran, Iran
Marvasti@sharif.edu

SJ Heydari and A Golmohammadi, A Kazerouni, MM Khalili
ACRI and EE Dept.
Sharif University of Technology
Tehran, Iran

Abstract— **Classical sampling theorem states that by using an anti-aliased low-pass filter at the Nyquist rate, one can transmit and retrieve the filtered signal. This approach, which has been used for decades in signal processing, is not good for high quality speech, image and video signals where the actual signals are not low-pass but rather sparse. The traditional sampling theorems do not work for sparse signals. Modern approach, developed by statisticians at Stanford (Donoho and Candes), give some lower bounds for the minimum sampling rate such that a sparse signal can be retrieved with high probability. However, their approach, using a sampling matrix called compressive matrix, has certain drawbacks: Compressive matrices require the knowledge of all the samples, which defeats the whole purpose of compressive sampling! Moreover, for real signals, one does not need a compressive matrix and we shall show in this invited paper that random sampling performs as good as or better than compressive sampling. In addition, we show that greedy methods such as Orthogonal Matching Pursuit (OMP) are too complex with inferior performance compared to IMAT and other iterative methods. Furthermore, we shall compare IMAT to OMP and other reconstruction methods in term of complexity and show the advantages of IMAT. Various applications such as image and speech recovery from random or block losses, salt & pepper noise, OFDM channel estimation, MRI, and finally spectral estimation will be discussed and simulated.**

Keyword: IMAT; sparse; OMP; OFDM Channel Estimation, Spectral Estimation, Salt&Pepper and clippling Noise, MRI

I. INTRODUCTION

In this invited paper, we would like to show the advantages of iterative thresholding for the recovery of sparse signals for various applications such as Salt & Pepper noise removal, nonuniform sampling of biomedical images, spectral and channel estimation. Our main contention is that the proposed iterative methods are faster and much less complex than the compressed sensing approaches such as Orthogonal Matching Pursuit (OMP).

II. ITERATIVE METHOD WITH ADAPTIVE THRESHOLDING (IMAT)

IMAT was first introduced in [1] and [2]. Despite of most of the existing reconstruction methods which are designed to deal with 1-D signals, IMAT can be easily adapted to be used for 2 and 3-D signals. Figure 1. depicts the steps of IMAT in details.

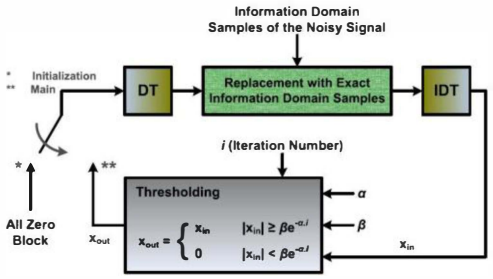

Figure 1. Block diagram of IMAT

In this block diagram, the DT and IDT blocks are Discrete Transform and its inverse, respectively. Let x be a sparse signal in an arbitrary domain (B1) where we have a subset of its samples in another domain (B2). The DT block is used for transforming the signal from the sparsity domain (B1) to information domain (B2). To initialize, the signal is estimated as an all-zero block. Then, the estimated signal is transformed into information domain (B2), and the samples are replaced. Next, the signal is sparsed using an adaptive thresholding filter which does not pass the components below a specific threshold value. In order to retrieve all the coefficients of the signal, the threshold is set to a large value at first and decays exponentially as the iteration number increases. After a number of iterations, the estimated signal becomes more similar to the original one.

III. SPARSE SIGNAL PROCESSING USING IMAT

In this section, various applications of IMAT are illustrated and the simulation results are presented.

A. Comparison of IMAT with OMP

In this subsection, we thoroughly investigate the performance of IMAT for signal compression and Compressed Sensing (CS) [3], [4] and illustrate its superiority to the popular sparse recovery method coined as Orthogonal Matching Pursuit (OMP) [5]. The sampling process used in IMAT differs from that of the ordinary CS recoveries. IMAT takes random samples of the signal by applying a simple binary mask to the image. While sampling in the ordinary CS is done by taking linear combinations of the signal coefficients using measurement matrices which should satisfy special constraints like low mutual coherence or the so-called Restricted Isometry

978-1-4673-0747-5/12/$31.00 ©2012 IEEE

Property (RIP) [6] to guarantee an exact recovery with a high probability.

For the first simulation, the two methods are applied for the recovery of compressively sampled image. As the complexity burden of OMP increases with the size of the signal, this algorithm should be applied to non-overlapping blocks of the image separately. To have a fair comparison, we use the same procedure for IMAT. Since OMP is designed for 1-d signals, each image block should be vectorized, e.g., row by row or column by column. However, IMAT can sample the 2-d signals directly by exploiting 2-d mask. Hence, IMAT, unlike OMP can exploit the spatial correlation of the image using 2-d transforms. The simulation time can be considered as a measure for the complexity of the methods. Figure 2. and 3, respectively, depict the simulation time and PSNR of the two methods (OMP and IMAT) versus the block size.

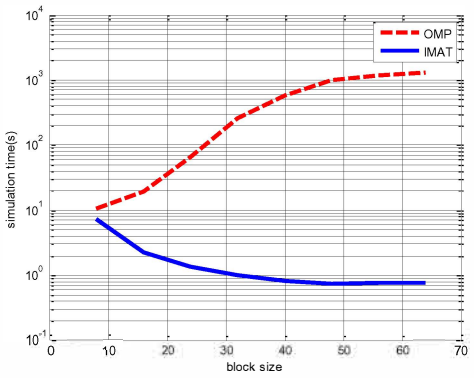

Figure 2. The simulation time versus block size for the baboon image

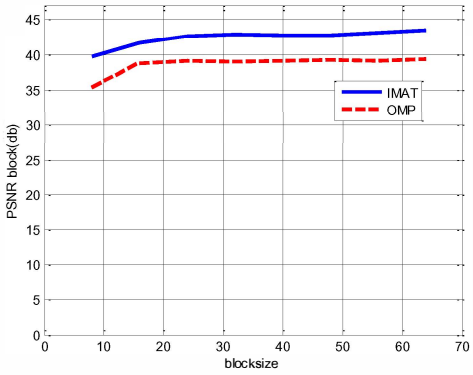

Figure 3. PSNR versus block size for baboon image

According to these figures, the simulation time of IMAT decreases with increasing the block size while its performance improves slightly. Therefore, we can use IMAT for the whole image. In the case of OMP method, although the performance of OMP improves for larger block sizes, it takes an intolerable amount of simulation time. The block size of 8×8 provides a tradeoff between the performance of OMP and its simplicity. For this block size, the averaged PSNR over 10 iterations has been depicted versus the sampling rate in Figure 4.

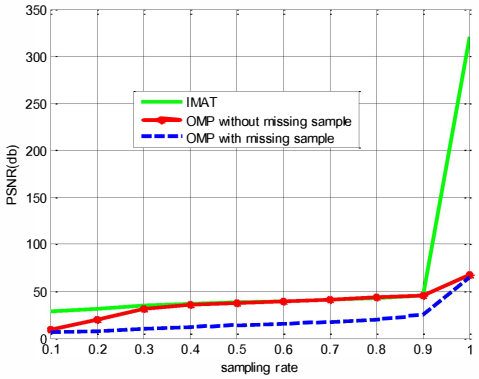

Figure 4. PSNR versus sampling rate for baboon image

As it can be seen, the PSNR of the recovered image using the IMAT method is higher than that of OMP. In the simulations, the IMAT method is applied for recovering a signal from random samples. On the other hand, the OMP method utilizes a linear combination of all the signal coefficients. In order to have a fair comparison with the IMAT, we should only use the OMP method with a sparse matrix that combines only random samples. Figure 4. shows the OMP with random samples. According to this figure, the performance of OMP degrades even further.

B. Iterative methods for random sampling

In this section, a number of iterative methods are described for random sampling. In the Iterative Hard Thresholding (IHT) [7] method, a certain number (the sparsity number) of the largest coefficients of the DFT representation of the signal are selected at each iteration. After performing the inverse DFT, non-distorted samples of the received signal are replaced in the information domain signal. The modified IHT method is very similar to the IHT method. The only difference is that at the i_{th} iteration of the modified IHT method, all of the DFT coefficients of the signal except the i_{th} largest are set to zero. After a number of iterations, the original signal can be recovered without having any knowledge of the sparsity of the underlying signal. The other iterative method simulated here is the modified IMAT. At each iteration of this method, the algorithm selects a variable number, P, of largest coefficients of the signal, where

$$P = \begin{cases} k1 + i \times k2 & i < K \\ K & otherwise \end{cases}. \qquad (1)$$

where i is the iteration number. The parameters k1, k2 and K are selected by trial and error. In this work, we have set k1, k2 and K to 5000, 700, 15000, respectively. The simulation results of various reconstruction methods for the baboon image are depicted in Figure 5. As IHT method needs sparsity number for successful reconstruction, the image is sparsed with a rate of 50%, *i.e.* 50% of its FFT coefficients are set to zero for IHT to work. For the other methods, no pre-processing of the image is needed.

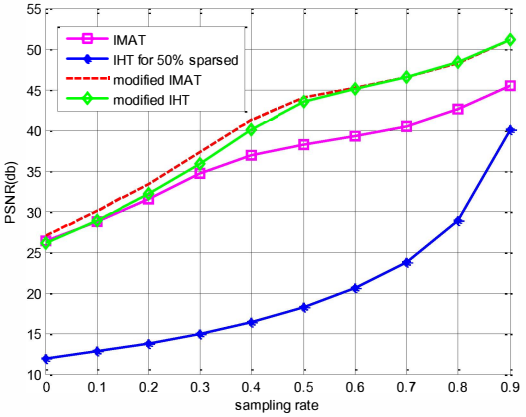

Figure 5. PSNR of IMAT, modified IHT, and modified IMAT versus sampling rate for the baboon image.

According to this figure, the modified IMAT and modified IHT exhibit similar performances which are slightly better than that of IMAT for higher percentage rates. IHT seems to be the worst.

C. *MRI Reconstruction using IMAT*

In this subsection, we will address the problem of Magnetic Resonance Image (MRI) reconstruction and provide the details of how this can be tackled by IMAT. In MRI, the reconstruction problem corresponds to the computation of the image from an incomplete set of its samples in the Fourier domain. In fact, according to some predefined sampling patterns, the Fourier samples of the image are obtained by applying a strong static magnetic field and a radio frequency magnetic field on a subject. The samples of the image in the Fourier domain are then mapped to the Cartesian grid [8][9]. The sampling pattern is usually either spiral or radial which cause the reconstruction procedure to be more accurate. For practical reasons, it is of crucial importance to decrease the sampling rate and increase the processing speed.

Consider X as the desired image to be reconstructed. Let Y be the 2-D Discrete Fourier Transform (DFT) of the image, i.e.,

$$Y = DFT(X) \tag{1}$$

The problem of MRI reconstruction can be stated as computing X from a number of samples of Y. The image signals have sparse representation in some well-known domains such as Discrete Cosine Transform (DCT) and various types of wavelets. Therefore, one can think of the sparse representation of the medical images in these domains. We consider Dual-Tree Complex (DTC) wavelet as the sparsity domain. Now, let Z be the DTC transform of X:

$$Z = \mathrm{DTC}(X). \tag{2}$$

From (1), we have:

$$X = \mathrm{IDFT}(Y) \tag{3}$$

where IDFT indicates the Inverse Discrete Fourier Transform. By replacing (3) into (2), one can write:

$$Z = \mathrm{DCT}(\,\mathrm{IDFT}(Y)\,). \tag{4}$$

Now, let Γ denote the composite transformation DTC o IDFT. Therefore, (4) can be written as:

$$Z = \Gamma(Y) \tag{5}$$

where, obviously Γ is an invertible linear function. On the other hand, according to (2):

$$X = \mathrm{IDTC}(Z) \tag{6}$$

where IDTC indicates the Inverse Dual-Tree Complex wavelet transform. Therefore, computing X out of Y is equivalent to obtaining Z from Y. From Compressed Sensing point of view and according to (5), Z is a sparse representation of Y. Our method is to find Z out of samples of Y by means of IMAT. In fact, Z is in the sparse domain and Y is in the information domain. The DT block (Figure 1. is the operation Γ as defined in (5). After finding Z, X can be easily obtained according to (6). We implemented our proposed method in various situations and compared it with other best-known existing algorithms. Figure 6. depicts the reconstruction result for image phantom the sampling pattern consists of vertical lines. This figure confirms the capability of proposed method in low sampling rates.

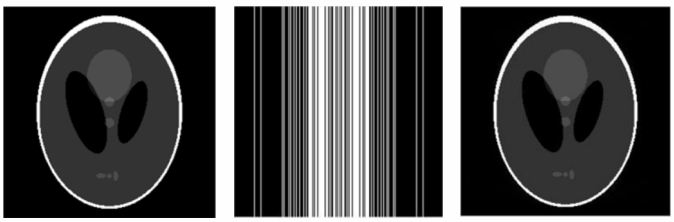

Figure 6. Reconstruction of Phantom image from sparse sample: (a) original image, (b) sampling mask,(c) reconstructed image.

In Figure 7. , our method is compared to the original image. In this case, the sampling pattern is radial and the simulations are performed for image phantom. As depicted in this figure, our method performs very well.

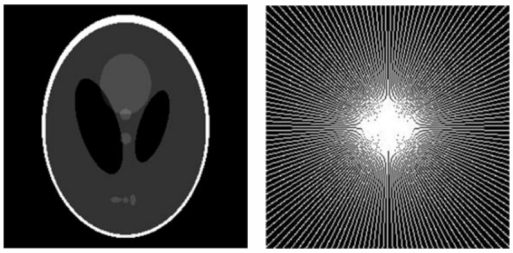

a)original image b)radial mask

e) IMAT

Figure 7. Image reconstruction from sparse samples using IMAT.

D. *Salt-and-Pepper noise removal based on IMAT*

In this subsection, the application of IMAT in image denoising is illustrated. Salt-and-Pepper is a common noise that corrupts images during the acquisition procedure or transmission through communication channels. This kind of noise affects the image by changing the value of a percentage of pixels to minimum or maximum available magnitude. Let X be a noise-free image, and Y be the noisy image. The Salt-and-Pepper noise can be modeled as:

$$Y=X+N \tag{7}$$

The matrix N indicates the salt-and-pepper noise that changes the value of some pixels of X. The problem here is to recover X from Y [1]. We can exploit the sparsity of the images to remove their noise. We consider the DTC wavelet as the DT transform introduced in IMAT. The problem of recovering an image from its salt-and-pepper noisy version is equivalent to a sparse signal recovery problem. Suppose that Y is the noisy version of an image as defined in (7). The noise free pixels of Y are the ones whose amplitudes are unequal to the maximum or minimum allowed value. Thus, the position and amplitude of noise free pixels are known. The noise-free image, X can be reconstructed by applying the IMAT algorithm to the noisy image defined by Y. The noise free pixels of Y are the information domain samples which are substituted in each iteration of the IMAT algorithm. To show the power of the IMAT in image denoising, this algorithm is applied to Lena corrupted with Salt-and-Pepper noise with different values of noise percentage. The simulation results of the proposed method are compared with other reconstruction methods such as Adaptive Median Filter (AMF) [9], Progressive Switching Median Filter (PSMF) [10], Detail-Preserving Median Filter (DPMF) [11], Decision-Based Algorithm (DBA) [12], Edge-Preserving Algorithm (EPA) [13], Switching-based Adaptive Weighted Mean filter (SAWM), Iterative Mean filter (AIM) in Figure 8.

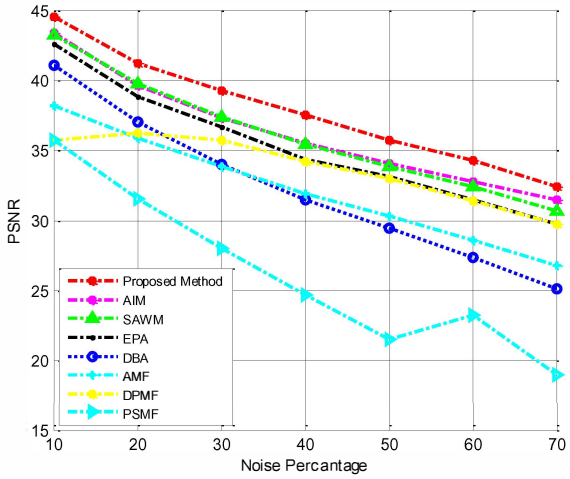

Figure 8. PSNR of different denoising methods for Lena image

E. *Spectral Estimation*

In this section, we show how IMAT performs in evaluating the sparse frequency contents of a signal [14][15][16][17]. Signal spectrum estimation methods are dependent on the features of the signal. For example, some methods can be used for wideband signals while others are useful for narrowband ones. Non-parametric methods, like periodogram, are robust with low complexity, but their resolution is low; consequently, parametric methods, which make some assumptions about signal, are desirable. Some classic methods, such as Prony, Pisarenko and MUltiple SIgnal Classification (MUSIC), have an acceptable performance under some conditions. For example, the Prony method performs well in noiseless cases and Pisarenko has a better performance at the presence of noise, while MUSIC outperforms both of them in noisy conditions. MUSIC is a method originally devised for high resolution source direction estimation in the context of array processing [2]. MUSIC can be understood as a generalization and improvement of the Pisarenko method. In the Pisarenko method, we assume a one dimensional subspace to noise [17], while in MUSIC, we extend this method, using a noise subspace of dimension greater than one to improve the performance. We also use some kind of averaging over noise eigenvectors to obtain a more reliable signal estimator. The data model for the sum of exponentials plus noise can be written as:

$$y_{m\times 1} = A_{m\times k} b_{k\times 1} + n_{m\times 1} \tag{8}$$

where m is the number of observed samples and k is the parameter of sparsity, n is the noise vector and y is the observation vector. The correlation matrix of the observation is given by:

$$R = Abb^H A^H + \sigma^2 I \tag{9}$$

where the noise is assumed to be white with variance σ^2. If we decompose R into its eigenvectors, k eigenvalues corresponding to the k-dimensional subspace of the first term

of the above equation are essentially greater than the remaining m – k values, σ^2, corresponding to the noise subspace; thus, by sorting the eigenvalues, the noise and signal subspaces can be determined. Assume ω is an arbitrary frequency and $\mathbf{e}(\boldsymbol{\omega}) = [1, e^{j\omega}, \ldots, e^{j(m-1)}]$. The MUSIC method estimates the spectrum content of the signal at frequency ω by projecting the vector e(ω) into the noise subspace. When the projected vector is zero, the vector e(ω) falls in the signal subspace and most likely, ω is among the spectral tones. In fact, the frequency content of the spectrum is inversely proportional to the L_2-norm of the projected vector:

$$P_{MU}(\omega) = \frac{1}{\boldsymbol{e}^H(\omega) \prod \boldsymbol{e}(\omega)} \tag{10}$$

$$\prod = \sum_{i=k+1}^{m} v_i v_i^H \tag{11}$$

where vi s are eigenvectors of R corresponding to the noise subspace. The k peaks of PMU(ω) are selected as the frequencies of the sparse signal. The determination of the number of frequencies (model order) in MUSIC is based on the Minimum Description Length (MDL) and Akaike Information Criterion (AIC) methods. In Figure 9. we compared the Mean Squared Error (MSE) of both methods as a function of SNR.

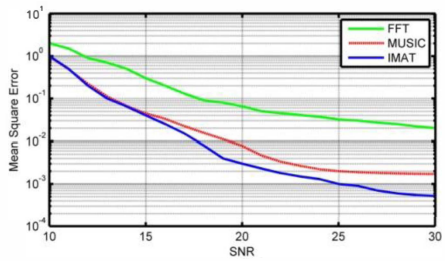

Figure 9. A comparison of the MSE of various spectral estimation methods.

It was shown that, the MUSIC method performs better than a simple Fast Fourier Transform (FFT) while the IMAT outperforms both for any noise levels. Moreover, the MUSIC approach needs eigenvalue-decomposition which makes it more complex and its implementation is difficult. The IMAT only needs a hard threshold which makes it simpler. As a result, IMAT is attractive for spectral estimation.

F. OFDM Channel Estimation Using Channel Sparsity

The problem of multipath channel distortion arises in all wireless communication systems where the transmitted signal is reflected from many scattering objects. This phenomenon causes the received signal to be a mixture of reflected and scattered versions of the transmitted signal. That is:

$$h(t,\tau) = \sum_{l=0}^{k-1} \alpha_l(t)\delta(\tau - \tau_l(t)) \tag{13}$$

where k is the number of taps, α_l is the l^{th} complex path gain, and τ_l is the corresponding path delay. In OFDM systems, the sampled version of channel impulse response in (13) presented in the DFT domain becomes:

$$H[r,i] \triangleq H(rT_f, i\Delta f) = \sum_{l=0}^{n-1} h[r,l] e^{-\frac{j2\pi il}{n}} \tag{14}$$

$$h[r,l] = h(rT_f, iT_s) \tag{15}$$

where T_f and n are the symbol length (including cyclic prefix) and the number of subcarriers in each OFDM symbol, respectively. Δf is the sub-carrier spacing and $T_s = 1/\Delta f$ is the sample interval. The above equation shows that for the r^{th} OFDM symbol, H[r, i] is the DFT of h[r, l].

Our goal in OFDM Channel estimation is to estimate the frequency response in (14) at each time slot of transmission. In other words, the channel frequency response should be estimated from the noisy values of the received samples at the pilot subcarriers. That is equivalent to solving the following equation for

$$\widetilde{H}_{i_p} = F_{i_p} h + \vartheta_{i_p} \tag{16}$$

where i_p is an index vector denoting the pilot positions in the frequency spectrum, $\widetilde{\boldsymbol{H}}_{i_p}$ is a vector containing the noisy values of the channel frequency spectrum in these pilot positions, and $\boldsymbol{F}_{i_p}$ denotes the matrix obtained from taking the rows of the DFT matrix pertaining to the pilot positions. $\boldsymbol{\vartheta}_{i_p}$ is the additive noise on the pilot points in the frequency domain. There is a vast literature on different estimation methods [19] to solve (16). The Least Square (LS) [19], Maximum Likelihood (ML) [20], Minimum Mean Squared Error (MMSE) [21], and Linear Minimum Mean Squared Error (LMMSE) [21], [22] techniques are among some of these methods. However, these methods do not exploit the inherent sparsity of the channel impulse response, therefore, they are not as exact. Therefore, we present a version of IMAT for OFDM channel estimation [23] which exploits channel sparsity to improve the accuracy of estimation and investigate its efficiency through a set of simulations. We apply our IMAT method to estimate OFDM channels formulated in (16). The main goal is to estimate $\boldsymbol{h}$ from $\widetilde{\boldsymbol{H}}_{i_p}$ given that $\boldsymbol{h}$ has a few non-zero coefficients. To achieve our goal, we need an initial crude estimate $\widehat{\boldsymbol{h}}_0$, and a set of iterations with adaptive thresholding to remove fake taps. As the initial estimate, we use the pseudo-inverse of $\boldsymbol{F}_{i_p}$ which yields a solution with minimum l_2-norm:

$$\begin{aligned}\widehat{\boldsymbol{h}}_0 &= \boldsymbol{F}_{i_p}{}^{+} \widetilde{\boldsymbol{H}}_{i_p} = \boldsymbol{F}_{i_p}{}^{+} \boldsymbol{F}_{i_p} \boldsymbol{h} + \boldsymbol{F}_{i_p}{}^{+} \boldsymbol{\vartheta}_{i_p} \\ &= \underbrace{\frac{1}{N} \boldsymbol{F}_{i_p}{}^{H} \boldsymbol{F}_{i_p}}_{\boldsymbol{G}_{N\times N}} \boldsymbol{h} + \frac{1}{N} \boldsymbol{F}_{i_p}{}^{H} \boldsymbol{\vartheta}_{i_p}\end{aligned} \tag{17}$$

Where we used

$$\boldsymbol{F}_{i_p}{}^{+} = \boldsymbol{F}_{i_p}{}^{H} \underbrace{(\boldsymbol{F}_{i_p} \boldsymbol{F}_{i_p}{}^{H})^{-1}}_{\frac{1}{N}\boldsymbol{I}_{N_p\times N_p}} = \frac{1}{N} \boldsymbol{F}_{i_p}{}^{H} \tag{18}$$

The non-zero coefficients of h are found through a set of iterations presented in (19) followed by adaptively decreasing thresholds:

$$\widetilde{\boldsymbol{h}}_k = \lambda\left(\widehat{\boldsymbol{h}}_0 - \boldsymbol{G}.\widehat{\boldsymbol{h}}_{k-1}\right) + \widehat{\boldsymbol{h}}_{k-1} \tag{19}$$

$$\widehat{\boldsymbol{h}}_k(i) = \begin{Bmatrix} \widetilde{\boldsymbol{h}}_k(i) & \left|\widetilde{\boldsymbol{h}}_k(i)\right| > \beta e^{-\alpha i} \\ 0 & otherwise \end{Bmatrix} \quad (20)$$

where λ and k are the relaxation parameter and the iteration number, respectively, and $G = \frac{1}{N} {F_{i_p}}^H F_{i_p}$ as defined in (18). We conduct simulations to compare IMAT with other algorithms in OFDM channel estimation process. For OFDM simulations, the DVB-H standard was used with the 16-QAM constellation in the 2K mode (2^{11} FFT size). The channel profile was the Brazil channel D. Figure 10. Shows the Symbol Error Rate (SER) versus the SNR after equalizing using different sparse reconstruction methods such as conventional linear interpolation, OMP, Compressive Sampling (CoSaMP) [24], Gradient Projection for Sparse Reconstruction (GPSR) [25] and our proposed IMAT.

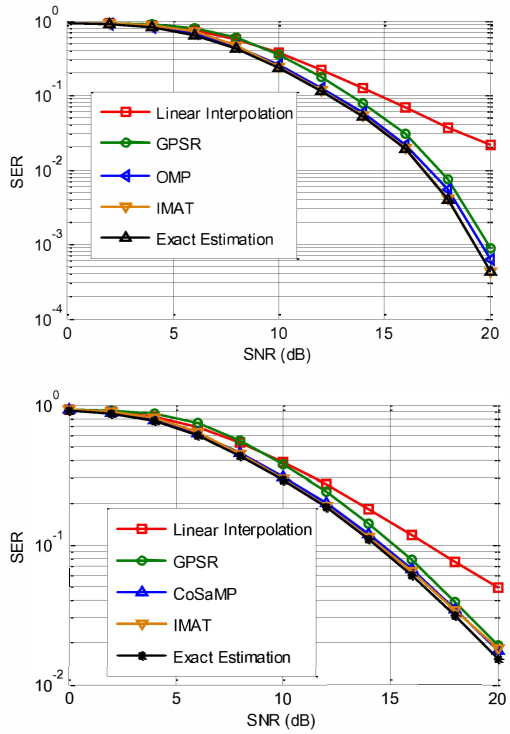

Figure 10. Comparison of SER (Symbol Error Rate) vs. SNR for conventional and sparsity based OFDM channel estimation methods and the IMAT for the Brazil channel at $F_d = 0$Hz (up) and $F_d = 50$Hz (down)

As we see in Figure 10. , IMAT is able to almost perfectly (relative to ideal channel estimation case) estimate channel impulse response compared to other estimation methods.

REFERENCES

[1] R.Eghbsli , A.Kazerooni , A.Rashidinejad and F.Marvasti, " Iterative method with adaptive thresholding for sparse signal reconstruction," International Workshop on Sampling Theory and Applications (SampTA) , Singapore, May 2011.

[2] F. Marvasti, A. Amini, F. Haddadi, M. Soltanolkotabi, et al, "A Unified Approach to Sparse Signal Precessing" Arxiv preprint, arXiv: 0902.1853v1, Feb 2009.

[3] E. J. Candès and M. B. Wakin, "An introduction to compressive sampling," IEEE Signal ProcessingMagazine, vol. 25, no. 2, pp. 21–30, March 2008.

[4] D. L. Donoho, "Compressed sensing," IEEE Transaction on Information Theory, vol. 52, no.4,pp. 1289–1306, April 2006.

[5] J. A. Tropp and A. C. Gilbert, "Signal recovery from partial information via orthogonal matching pursuit," IEEE Transaction on Information Theory, vol. 53, no.12, pp. 4655–4666, December 2007.

[6] E. J. Candes, J. K. Romberg, and T. Tao, "Stable signal recovery from incomplete and inaccurate measurements," Communications on Pure and Applied Mathematics, vol. 59, no. 8, pp. 1207-1223, 2006.

[7] T. Blumensath and M. E. Davies, "Iterative Hard Thresholding for Compressed Sensing," (2009) Applied and Computational Harmonic Analysis, vol. 27(3), pp. 265–274, April 2009.

[8] H.Schomberg and J.Timmer ,"The gridding method for image reconstruction by Fourier transformation," IEEE Transactions. Med.Image , vol.14, no.3, pp.596-607 , 1995

[9] P. E. Ng and K. K. Ma, "A switching median filter with boundary discriminative noise detection for extremely corrupted images," IEEETrans. on Image Process, vol. 15, no. 6, pp. 1500–1516, June 2006.

[10] Z. Wang and D. Zhang, "Progressive switching median filter for theremoval of impulse noise from highly corrupted images," IEEE Trans. on Circuits and Systems II, vol. 46, pp. 78–80, 1999.

[11] W. Li, Y. Sun, and S. Chen, "A new algorithm for removal of highdensity salt and pepper noises," IEEE Conference on Image and signal processing,(CISP), 2009.

[12] K. S. Srinivasan and D. Ebenezer, "A new fast and efficient decisionbased algorithm for removal of high density impulsive noise," IEEE Signal Processing Lett., vol. 14, no. 3, pp. 189–192, March 2007.

[13] P. Y. Chen and C. Y. Lien, "An efficient edge-preserving algorithm for removal of salt and pepper noise," IEEE Signal Process. Lett., vol. 15, pp. 833–836, December 2008.

[14] S. L. Marple, Digital Spectral Analysis. Prentice-Hall, Englewood Cliffs, NJ, 1987.

[15] S. M. Kay and S. L. Marple, "Spectrum analysis-a modern perspective," Proc. IEEE, Reprinted by IEEE Press, (Modern Spectrum Analysis II), vol. 69, no. 11, pp. 1380–1419, Nov. 1981.

[16] S. M. Kay, Modern Spectral Estimation: Theory and Application. Prentice-Hall, Englewood Cliffs, N.J., Jan. 1988.

[17] P. Stoica and R. L. Moses, Introduction to Spectral Analysis. Upper Saddle River, NJ: Prentice-Hall, 1997.

[18] P. Stoica and A. Nehorai, "Music, maximum likelihood, and Cramer-Rao bound," IEEE Trans. on ASSP, vol. 37, no. 5, pp. 720–741, May 1989.

[19] J. J. V. de Beek, O. Edfors, M. Sandell, S. K. Wilson, and P. Borjesson, "On channel estimation in OFDM systems," Proc. 45th IEEE Vehicular Technology Conf., Chicago, vol. 2, pp. 815-819, Jul. 1995.

[20] M. Morelli and U. Mengali, "A comparison of pilot-aided channel estimation methods for OFDM systems," IEEE Trans. on Signal Proc., vol. 49, no. 12, pp. 3065-3073, Dec. 2001.

[21] O. Edfors, M. Sandell, J.-J. V. de Beek, and S. K. Wilson, "OFDM channel estimation by singular value decomposition," IEEE Trans. on Comm., vol. 46, no. 7, pp. 931-939, July 1998.

[22] S. G. Kang, Y. M. Ha, and E. K. Joo, "A comparative investigation on channel estimation algorithms for OFDM in mobile communications," IEEE Trans. on Broadcasting, vol. 49, no. 2, pp. 142-149, June 2003.

[23] P. Pakrooh, A. Amini, and F. Marvasti, "OFDM Pilot Allocation for Sparse Channel Estimation," To Appear in Eurasip Journals on Advances in Singal Processing. Arxiv preprint arXiv:1106.4507, 2011.

[24] . D. Needell and J. A. Tropp, "Cosamp: iterative signal recovery from incomplete and inaccurate samples," App. and Comp. Harmonic Analysis, vol. 26, pp. 301-321, May 2009.

[25] M. A. T. Figueiredo, R. D. Nowak, and S. J. Wright, "Gradient projection for sparse reconstruction: Application to compressed sensing and other inverse problems," IEEE Journal on Selected Topics in Signal Proc., vol. 1, no. 4, pp. 586-597, Dec. 2007.